PHILOSOPHICAL TRANSACTIONS A

Phil. Trans. R. Soc. A.

doi:10.1098/not yet assigned

Nitrogen Concentration Control during Diamond Growth for NV⁻ Center Formation

T. Teraji[1,*] , C. Shinei[1], Y. Masuyama[2], M. Miyakawa[3], T. Taniguchi[3]

[1] *Research Center for Electronic and Optical Materials, National Institute for Materials Science, 1-1 Namiki, Tsukuba, Ibaraki 305-0044, Japan*

[2] *Quantum Materials and Applications Research Center, National Institutes for Quantum Science and Technology, 1233 Watanuki-machi, Takasaki, Gunma, 370 – 1292, Japan*

[3] *Research Center for Materials Nanoarchitectonics (MANA), National Institute for Materials Science, 1-1 Namiki, Tsukuba, Ibaraki 305-0044, Japan*

Keywords: diamond, HPHT, CVD, nitrogen, doping, NV center,

Abstract

Negatively charged nitrogen-vacancy (NV^-) centers formed in diamond crystals are point defects that have potential applications in various quantum devices such as highly sensitive magnetic sensors. To improve the sensitivity of magnetic sensors using NV^- centers, it is essential to precisely control the nitrogen concentration in the crystals. In this paper, we demonstrated that nitrogen concentration in diamond can be controlled with high precision for the following two representative growth methods. One is the high-pressure high-temperature (HPHT) synthesis method and the other is chemical vapor deposition (CVD) method. The nitrogen concentration of HPHT-grown diamond decreased semi-logarithmically with increasing contents of titanium or aluminum as nitrogen getter materials. The nitrogen concentration of CVD-grown diamond increased linearly with increasing the flow rate ratio of nitrogen to carbon. NV^- centers were formed by controlling the total fluence of electron beams so that approximately 20% of the nitrogen became NV^- centers. The coherence time of electron spin of NV^- centers obtained by the Hahn-echo pulse sequence T_2 of these diamond crystals was inversely proportional to the nitrogen concentration. A comparison of T_2 of the NV^- centers for HPHT-synthesized and CVD-grown diamonds showed no significant difference between them.

1. Introduction

Recently, the term "quantum technology" has become increasingly common [1]. The term "quantum technology" includes not only research into understanding quantum mechanical effects such as quantum

*Author for correspondence (TERAJI.Tokuyuki@nims.go.jp).

entanglement and quantum superposition, but also technologies that make use of these features, such as quantum computers, quantum communications, and quantum sensing. Currently, research and development for the practical application of these technologies is progressing rapidly around the world [2, 3].

Quantum sensing is one of the major technical areas of quantum technology, and negatively-charged nitrogen-vacancy centers (NV^- centers) formed in diamond crystals have attracted much attention [4, 5]. Quantum sensor based on NV^- centers can operate at room temperature. In addition, the NV^- center can be expected to have high spatial resolution because the sensor cell (NV^- center body) is as small as the atomic scale, and high sensor sensitivity can be expected because the sensor can be placed close to the target [6, 7, 8, 9, 10]. Because of these unique features of the NV^- center, many universities and research institutes around the world are currently conducting basic and practical research on solid-state quantum sensors with room-temperature operation and high spatial resolution using the NV^- centers.

NV^- centers have long been known as one of the typical optical centers (color centers) that form in diamond crystals. And since a German research group reported electron spin resonance (optically detected magnetic resonance: ODMR) of a single NV^- center at room temperature in 1997 [11, 12], this point defect has attracted worldwide attention as a new quantum defect. NV^- centers are defect complex consisting of one substitutional nitrogen and one atomic vacancy. In order to obtain excellent electron spin properties (e.g., spin coherence time), the mother material, diamond, must have high crystallinity [13]. And since only the negatively charged NV center (NV^- center) can control the spin state, a high stability of negative charge state of the NV^- center is essential, which requires the removal of acceptor impurities as much as possible. In addition, paramagnetic defects in the diamond crystal must be reduced to have long coherent time of electron spin. Furthermore, since the spin state of the NV^- center is read from the fluorescence intensity, background light must be reduced for accurate reading, and luminescent centers other than the NV^- center must be removed from diamond crystals as much as possible. There is thus a demand on the material side for the diamond that forms the NV^- centers [13]. Therefore, the establishment of diamond crystal growth technology suitable for quantum devices is indispensable for improving device performance.

In this paper, we describe a diamond crystal growth technique and the formation method of NV^- center in diamond crystals for quantum sensing applications using NV^- centers, focusing on research results at the National Institute for Materials Science (NIMS). In particular, we discuss the controllability of nitrogen concentration in diamond by nitrogen doping during diamond growth.

2. Diamond growth technology

There are two methods for growing diamond crystals: high-pressure high-temperature synthesis (HPHT) and chemical vapor deposition (CVD) methods. In this chapter, we briefly review these growth methods and describe the current state of research on nitrogen doping.

(a) Growth method 1: High-pressure/high-temperature (HPHT) synthetic method

The HPHT method [14] is widely used for bulk crystal growth because diamond is thermodynamically stable under high pressure. More than 90% of lab-grown diamond is produced by the HPHT method [15], but high technology is required to grow high-purity single crystals free of impurities such as nitrogen, boron and solvent components. The HPHT method includes the temperature gradient method using a catalyst, the solubility difference method, the non-catalytic conversion method, and the shock compression method. Among these methods, the temperature gradient method is used to grow large, high-quality single-crystal diamonds. The details of this technique are described in the following references [16, 17].

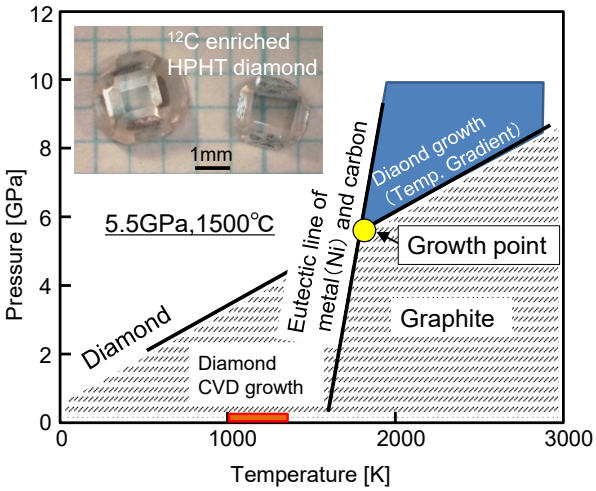

Figure 1. carbon phase diagram

Figure 1 shows a phase diagram of carbon, including the eutectic line of nickel and carbon. In the temperature gradient method, carbon materials are dissolved in a metallic solvent under high temperature and high pressure, and then precipitated as single crystals. During growth, it is necessary to control the growth parameters so that the temperature difference is several tens of degrees of centigrade between the part of the sample chamber where the raw material is dissolved (high temperature part) and the part where diamond is grown on seed crystals (low temperature part). Typical growth parameters are a pressure of 5.5 GPa or higher and a growth temperature of 1573 K (1300°C) or higher.

(b) Growth method 2: Chemical vapor deposition (CVD) method

For downsizing and generalization of diamond growth equipment, it is desirable to grow diamond under atmospheric pressure or low pressure. However, as shown in the phase diagram (Figure 1), diamond is a stable phase under high pressure, making it difficult to grow diamond under ambient pressure. In the early 1980s, the same institute (former national institute for research in inorganic materials NIRIM) proposed two well-known representative diamond CVD growth methods [18], which are the hot-filament CVD method [19] and the microwave plasma CVD method [20, 21]. Most of the diamond growth systems currently available on the market are based on these configurations.

The CVD method is a method for growing a thin film by supplying a source material gas containing constituent elements of the thin film into a reaction chamber. In this method, the source material gas is decomposed and a thin film is grown by chemical reaction on the substrate. When a thin

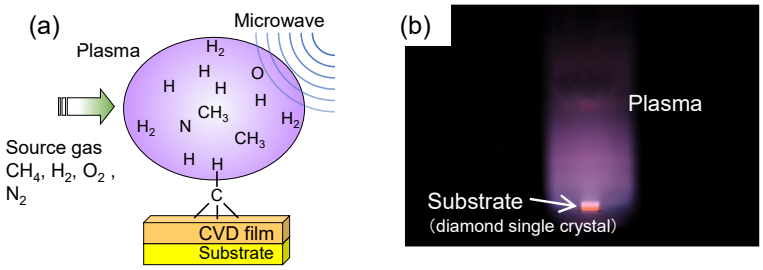

Figure 2. (a) Conceptual diagram of plasma CVD, (b) Appearance during microwave-plasma CVD growth

film is grown using a gas containing carbon as a source material, if the growth temperature is high, the substrate surface will be graphitized, making it impossible to grow diamond [22]. For this reason, the CVD method using non-equilibrium plasma is widely used in diamond thin film growth to reduce the substrate temperature (Figure 2(a), (b)). The details of the diamond crystal growth mechanism by this plasma-assisted CVD method are described in the following papers [23, 24]. Using diamond single-crystals as a substrate, it is possible to obtain functional single-crystal thin films with unique doping and stacking structures. In the past, "diamond single-crystal substrate" meant a single-crystal substrate synthesized by the HPHT method. Recently, improvements in the performance of CVD growth equipment have made it possible to grow diamond growth for long periods of time and free-standing CVD diamond wafers are also becoming available [25].

(c) Impurity doping of diamond

Diamond is a group IV semiconductor material with excellent physical properties. Until now, diamond crystals have been studied to improve their quality and purity, mainly for application in electronic devices such as power devices [25]. Doping with impurities that function as donors and acceptors is essential for the fabrication of semiconductor devices, and research is also being conducted on doping concentration control of these impurities. The small lattice constant of diamond limits impurities entering the diamond lattice [26]. Therefore, the elements that can be incorporated during the diamond growth process are limited. Nitrogen, boron, and phosphorus are typical elements as impurities that affect the Fermi level position of diamond. Regarding boron and phosphorus doping during CVD growth, there have been reports systematically demonstrating the growth parameter dependence of impurity concentrations over several orders of magnitude [25, 27]. On the other hand, there are few studies on such doping controllability for nitrogen. This is probably because, unlike boron and phosphorus, nitrogen forms deep electronic levels within the band gap and does not contribute to electrical conduction. Rather, it often has a detrimental effect on device properties, which is why research has focused on removing as much nitrogen as possible from diamond.

In HPHT synthetic diamond, about 50~500 ppm of nitrogen is incorporated spontaneously into the grown diamond. These nitrogen-doped diamonds exhibit a yellow color (type-Ib diamonds) [17]. The nitrogen probably comes from high pressure media surrounding the growth cell [16]. It is reported that metal solvent and temperature affect nitrogen incorporation into diamond, resulting in diamond with nitrogen concentrations below 50ppm [16, 28]. This has been interpreted in terms of the solubility of nitrogen in the metal solvent. A linear increase in nitrogen concentration from 2 ppm to 7 ppm was reported as the temperature increased from 1650 °C to 1850 °C [28]. In addition to the relatively small change in nitrogen concentration when changing synthetic temperature, it is not easy to control the temperature with good reproducibility in the long duration in HPHT diamond synthesis process [29]. Therefore, in this study, for the purpose of controlling the nitrogen concentration in a wide range, we have controlled nitrogen concentration by changing the weight ratio of nitrogen getter material in the metal solvent instead of changing synthetic temperature.

To reduce nitrogen concentration, nitride-forming metals such as titanium, aluminum and zirconium are frequently used as nitrogen getter materials [16]. It has been reported that the nitrogen content can be reduced below 0.1 ppm by this method [30]. The reduction of nitrogen content is also effective in reducing lattice distortion inside the crystal which is considered to be caused by inhomogeneous distribution of nitrogen [31]. On the contrary, the addition of NaN_3 to the metal solvent reportedly yields diamonds with nitrogen concentrations greater than 1000 ppm [32]. Nitrogen in HPHT diamond crystals has various point defect structures [14, 33]. The structure of nitrogen in diamond is predominantly substitutional nitrogen. Point defect complexes consisting of nitrogen atoms and vacancies are also formed. The emission wavelength from these

point defect complexes depends on the number of both nitrogen atoms and vacancies that make up these point defect complexes. The following point defect complexes are commonly observed from HPHT diamond crystals [16, 53]. The N3 center, composed of three nitrogen atoms and vacancies, has a zero-phonon line peak (ZPL) at 415 nm. The H3 center composed of two nitrogen atoms and a vacancy, and appears its ZPL at 503 nm. The NV centers are formed from pairs of nitrogen and vacancies, with ZPL of the NV^0 center appearing at 637 nm and ZPL of the NV^- center appearing at 575 nm. Irradiating the crystal with high-energy particles/electrons and then annealing the crystal enhances the intensity of these emissions [34].

In order to improve the crystalline quality of diamond, a method of using a seed crystal with few dislocations has been proposed [31]. By combining various quality improvement techniques, high-purity (type IIa) HPHT diamond with a diameter exceeding 10 mm and almost no dislocation defects in the (001) growth sector has been obtained at the research level [30]. The ^{13}C with nuclear spin (natural abundance ratio 1.1%) can be reduced by using ^{12}C isotope-enriched (^{13}C reduced) starting carbon materials. It has been reported that HPHT diamond single crystals with a ^{12}C isotopic concentration of 99.995% were obtained by using polycrystalline diamond films with a ^{12}C isotopic concentration of 99.998% as starting material [35].

In the CVD method, nitrogen doping increases the growth rate of diamond by about 2 to 10 times [24, 36, 37, 38], and diamond growth rate of greater than 100 μm h^{-1} have been reported [36, 39]. As such, the nitrogen doping techniques have been used to grow thick CVD diamond layers or free-standing CVD diamond plates. Nitrogen incorporation efficiencies during diamond growth reportedly range from 3×10^{-5} to 7×10^{-2}, which depend on growth conditions and nitrogen dopant gas. Here, the nitrogen incorporation efficiency is defined as the ratio of incorporated nitrogen in diamond crystal to the gas ratio of the nitrogen gas flow rate to the methane gas flow rate (N/C gas ratio) during CVD growth. Nitrogen molecular gas N_2 is often used as a dopant, but Tallaire *et al.*, proposed N_2O gas as a nitrogen dopant with high incorporation efficiency [40, 41]. The highest nitrogen concentrations are reportedly 35 ppm for free-standing CVD (001) plate [41] and 80 ppm for homoepitaxial (111) thin film [42]. Nitrogen doping frequently causes step bunching on the diamond (001) surface [36, 37, 43, 44, 45]. Chayahara *et al.*, reported that appearance of nonparaxial crystallites is suppressed by adding N_2 gas with few percent to methane [46], while Tallaire *et al.*, mentioned that addition of N_2 gas at concentration above a few tens of ppm induces the formation of extended or unepitaxial crystallites [41]. Nitrogen-doped CVD film exhibits brownish to dark coloration [40, 47], which might be attributable to the creation of vacancy clusters [48]. Nitrogen related point defects generated in CVD diamond crystals are mainly substitutional nitrogen in a neutral or positive charged state (N_s^0 and N_s^+), negatively or neutrally-charged NV center (NV^0 and NV^-) and NV^- center with hydrogen (NVH^- center) [37, 47, 58]. The concentration ratio of [N_s^0] (or [N_s^+]+ [N_s^0]) : [NVH^- center] : [NV^- center] is reportedly approximately 100 : 10 : 1 [37] or 300: 30: 1 [49]. There are limited reports showing the controllability of the nitrogen concentration in diamond, that is, the relationship between the nitrogen concentration in the diamond crystal and the doping gas concentration during CVD growth, and the control range of the nitrogen concentration is less than two orders of magnitude [37, 38].

(d) Preferential formation of NV^- centers

As mentioned above, quantum manipulation of electron spins at the NV^- center involves initializing and reading out the electron spin state by light irradiation and controlling (writing) the electron spin state by microwave irradiation. Required electron spin density (i.e., NV^- center density) varies depending on the spin control method [50] and device application [1051].

Even if diamond growth is performed with the purpose of forming only NV^- centers, defects other than NV^- centers will be formed in the actual diamond crystal at the same time (Figure 3(a)). In addition to threading

dislocation, defects such as atomic vacancies, interstitial carbon, hydrogen, and aggregate nitrogen [52, 53] may increase spin noise and reduce the formation rate of NV^- center. Therefore, they should be removed as much as possible from the crystal.

NV^0 centers capture negative charges and become negatively charged states (NV^-) with electron spins with spin quantum number S=1. Spin manipulation of NV^- centers is possible by applying microwave pulses, and magnetic sensitivity is improved by increasing the concentration of NV^- centers [NV^-]. On the other hand, the NV^0 center (S=1/2) cannot be spin-operated and becomes background light (noise). Therefore, increasing the negative charge stability of the NV^- centers is important for improving the magnetic sensitivity. In addition to NV^0 center, visible-region luminescent defects such as silicon vacancy (SiV^-) centers and H3 centers also act as background light, so it is important to remove them [53]. From the above, it can be understood that diamond crystals suitable for quantum devices must be grown based on high-purity crystal growth techniques.

Furthermore, in order to increase the coherence time of the electron spin of the NV^- centers, ^{13}C with nuclear spins (I=1/2) should be reduced. [54, 55]. Figure 3(b) shows an example of an ideal NV^- center formation state. Nitrogen takes a defect structure of NV^- center or isolated nitrogen in the neutral charge state (it is called N_s^0 or P1 center). Negative charges of NV^- centers are supplied from the N_s^0. In this sense, the optimum state is one in which [N_s^0] is slightly higher than [NV^-].

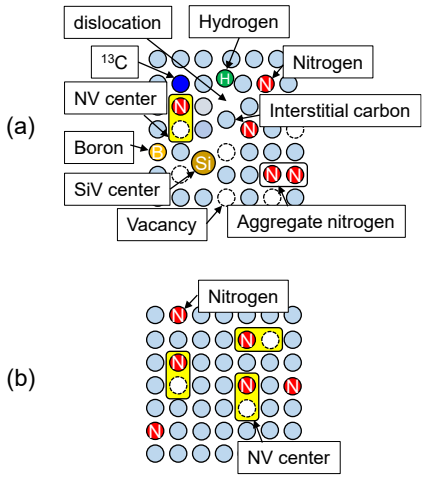

Figure 3. Formation of NV^- centers in diamond crystals (a) A realistic form with various impurities mixed in. (b) An ideal form consisting of NV^- centers and isolated nitrogen (donors).

3. Nitrogen-doped diamond growth

(a) Diamond growth conditions

In this study, growth of nitrogen-doped diamond crystals was performed by both HPHT and CVD methods. For the synthesis of diamond single crystals by the HPHT method, the temperature gradient method was used [29]. Diamond single crystal was grown on the (001) surface of the seed crystal, and Co-Ti, Fe-Co-Ti, and Co-Al (99.98%-99.999%, RARE METALLIC Co., Ltd.) were used as metal solvents. The HPHT condition is as follows; the growth temperature of 1300° C – 1350° C, the reaction pressure of 5.5 GPa, and the growth time of 40 – 80 hours. It has been reported that a Cu additive has the effect of suppressing the formation of TiC [56]. Therefore, in this study, Cu was added to the metal solvent when the Ti additive was used as a nitrogen getter material. We used a modified belt-type high-pressure apparatus [57]. The cylinder bore diameter is approximately 32 mm for the HPHT apparatus FB30H and is approximately 44 mm for the HPHT apparatus FB40H. Graphite (Tokai Kosho Co., Ltd.) was used as the carbon source in most of the diamond synthetic experiments in this study. On the other hand, for the growth of ^{12}C isotopically enriched HPHT synthetic diamond, ^{12}C-enriched CVD diamond (Tomei Diamond Corp.) was used because ^{12}C isotopically enriched graphite is not commercially available.

When the nitrogen concentration in the diamond crystal is less than 1 ppm, the effect of spin relaxation of the electron spin of the NV center by the electron spin of nitrogen is small. As a result, the perturbation from the nuclear spin of ^{13}C, whose natural abundance is 1.1%, to the coherence time T_2 of NV^- centers becomes non-negligible [13]. Therefore, in order to improve T_2 of NV^- centers, ^{12}C-enrichment has carried out for the

HPHT diamond crystals in the nitrogen doping range below 1ppm in this study. The grown single crystal was cut parallel to the {111} plane with a thickness of about 0.2 mm.

In the CVD method, nitrogen-doped homoepitaxial diamond film was grown by a microwave plasma CVD developed at National Institute for Materials Science (NIMS) [58]. Details of the microwave-plasma CVD system are described elsewhere [59, 60]. HPHT-grown type-Ib (100) diamond crystals with a dimension of 3.5 × 3.5 mm^2 in area and 1mm in thickness were used as substrates. Chemical purity of source gasses are 9N for hydrogen (using a palladium purifier), 8N for methane (using a zirconium purifier) and 6N5 for oxygen. ^{12}C isotopically enriched methane whose enrichment was specified to >99.9% was used as a carbon source gas. $^{15}N_2$ gas (chemical purity >3N) whose enrichment was specified to 98% were used as a nitrogen doping gas for samples 1–3. The CVD condition is as follows; the reaction pressure of 110 Torr, microwave power of 1.4 kW, methane concentration ratio (flow rate ratio of CH_4 to the total gas flow) of 10%, oxygen concentration (flow rate ratio of O_2 to the total gas flow) of 2% and substrate temperature of 1030–1090°C.

Microscope images of HPHT crystals and free-standing CVD diamond plates were obtained by using stereomicroscopes (SZ61; Olympus Co. Ltd.). Impurities in diamond crystals were characterized by secondary ion mass spectrometry (SIMS, IMS-7f; CAMECA, Ametek Inc.), electron paramagnetic resonance (EPR, JES-FA100, JEOL Ltd.), Fourier transform infrared (FTIR, FT/IR-6600, JASCO Co.) spectroscopy, and photoluminescence (PL, Nanofinder FLEX; Tokyo Instruments, Inc.) methods. The ^{12}C isotope enrichment of diamond crystals was evaluated by SIMS measurements.

(b) Grown crystals

Figure 4 shows how diamond {111} plates are prepared from crystals grown by the HPHT method. As-grown diamond crystals consist primarily of {100} and {111} growth sectors, as shown in Fig. 4(a). For the characterization of the quantum properties of NV^- centers, it is convenient to use {111} crystals because it is necessary to apply a magnetic field in the [111] direction. The {111} crystals are obtained by cutting an as-grown crystal into a plate shape in the direction shown in Fig. 4 (a). Two symmetrical plates can be cut out from one as-grown crystal. The crystals are generally 2−3 mm in size. The color of the {111} HPHT diamond crystals were almost colorless, as shown in Fig. 4(b). No contrast reflecting crystallographic strain was observed in the birefringent image, indicating that the strain was relatively small.

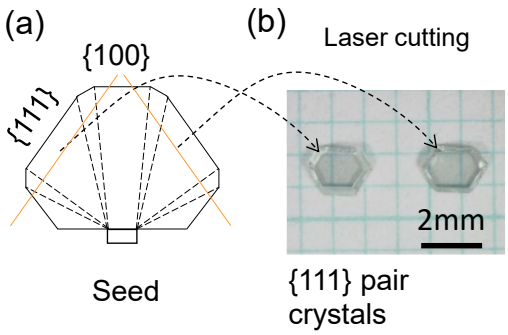

Figure 4. Method for preparing diamond {111} plates from crystals grown by the HPHT method

Figure 5 shows a microscope image of the as-grown state of CVD-grown diamond, taken in the brightfield reflection mode. The $^{15}N/C$ ratio in gas phase applied for the diamond growth of this sample was 20,000 ppm. Thickness of CVD layer was 430 μm. The step bunching described in subsection 2(c) was observed on the surface of the as-grown homoepitaxial film. Since defect formation was suppressed by the addition of oxygen in source gases, non-epitaxial crystallites and growth hillocks did not form on the diamond sample surface even after a prolonged growth. The blue dashed rectangle corresponds to the edge position of the substrate. Polycrystalline diamond was partially grown on the edges of the substrate.

To create freestanding CVD diamond (001) crystals, first, the top surface of the sample was laser-cut into a square shape to cut out the polycrystalline diamond portion, and then the sample was laser-cut from the side to remove the CVD layer from the substrate. Figures 5(b) and (c) show microscope images of the freestanding diamond sample taken in the brightfield reflection mode and birefringence image mode, respectively. The color of the diamond sample after being processed into a freestanding plate was relatively transparent, as shown in Fig. 5(b). Four-hold symmetric pattern was observed in the birefringence image, as shown in Fig. 5(c). This symmetric pattern reflects the {111} growth sector of HPHT crystals and is often observed in birefringence images of commercial HPHT-grown type-Ib (001) substrates. High density dislocations in the center part of sample also reflect the dislocation distribution of the HPHT substrate. It means that the strain of the free-standing plate is induced from the substrate and the crystal strain can be minimized by using a low-strain substrate. The isotopic enrichment of diamond crystals obtained from SIMS analysis was 99.96% for ^{12}C and more than 99.5% for ^{15}N [58]. These values meet the specification of these isotopically enriched gases used for the CVD diamond growth, indicating that the isotopic enrichment in the diamond crystals can be controlled by changing the isotopic enrichment of source gases.

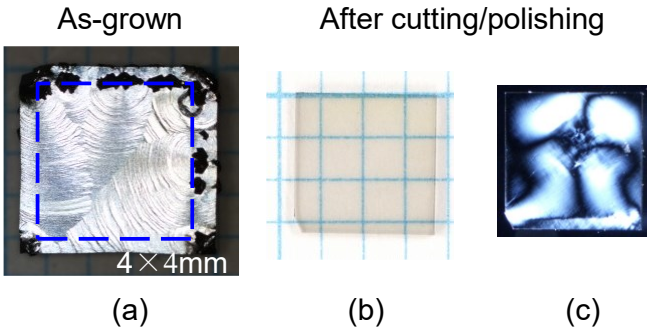

Figure 5. Optical microscope images of homoepitaxial diamond crystals. Brightfield reflection images of the sample (a) in an as-grown state and (b) after removal from the substrate. (c) Birefringence image of the sample after removal from the substrate (Reprinted from T. Teraji *et al.*, J. Appl. Phys **133**, 165101 (2023)).

(c) Nitrogen concentration

Figure 6 shows the concentration of substitutional nitrogen in the neutral charge state [P1] as measured by EPR measurements. Semi-logarithmic plot of [P1] for HPHT diamond samples as a function of Ti or Al addition [29]. [P1] was found to decrease exponentially with increasing Ti addition. When grown with Co-Ti solvent, [P1] was 100 ppm without Ti addition and about 1 ppm at Ti additive of 2.0 wt%. The variation of [P1] for the same Ti addition was about 100%. This variation is inferred to mainly come from the fact that different growth sectors have different nitrogen incorporation efficiency as explained below. Nitrogen

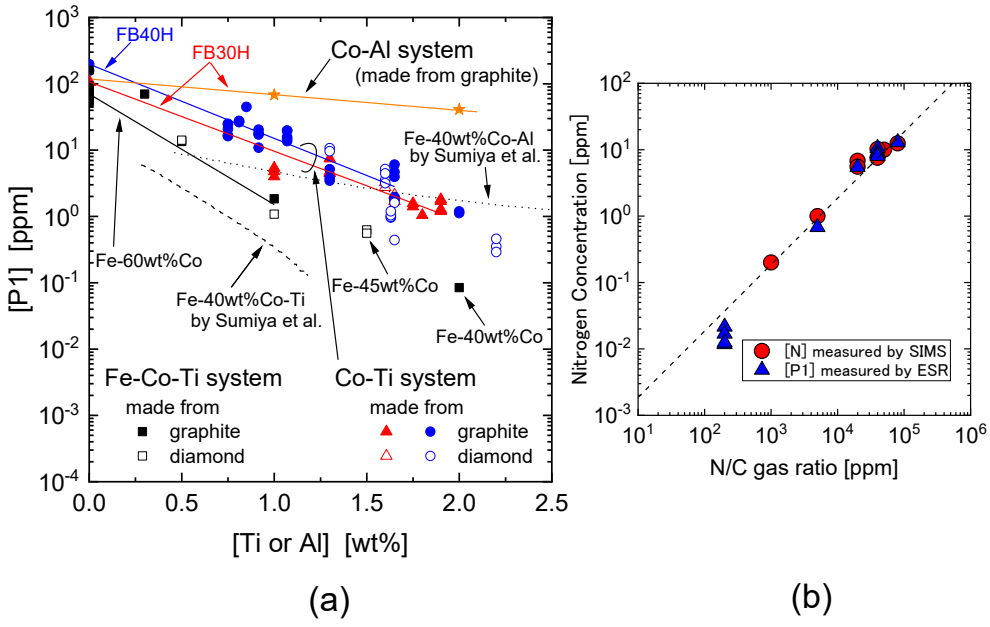

Phil.

Figure 6. Nitrogen concertation of diamond crystals. (a) diamond grown by HPHT method (Reprinted from M. Miyakawa *et al.*, Jpn. J. Appl. Phys **61**, 045507 (2022)., Copyright 2022 The Japan Society of Applied Physics, (b) diamond grown by CVD method (Reprinted from T. Teraji *et al.*, J. Appl. Phys **133**, 165101 (2023)).

concentrations are known to vary by growth sector within the crystal [14, 31]. In standard type-Ib synthetic diamonds, nitrogen concentrations of about 100 ppm in the {111} sector, less than 50 ppm in the {100} sector, less than 10 ppm in the {113} sector, and about 1 ppm in the {110} sector have been reported [61]. As shown in Fig. 4(b), the nitrogen concentration of HPHT crystals was evaluated using samples cut to center the {111} growth sector. The region of the {111} growth sector differs from sample to sample, and the rim of the sample is the growth sector with lower [P1] than that of {111} growth sector. [P1] of each sample is obtained by dividing the total number of electron spin of substitutional nitrogen of a sample by the sample volume. Variation in the proportion of the {111} growth sector in the overall sample is considered to be a cause of the variation in [P1] shown in Fig. 6 (a). When Al was used as a nitrogen getter material instead of Ti, [P1] was approximately 40 ppm at Al additive of 2.0 wt%. It means that Al also has a nitrogen getter effect, but its efficiency is lower than that of Ti. Therefore, more Al addition is necessary to control P1 concentration in the range of 0.1 to about 100 ppm [29].

In the case of CVD diamond, not only [P1] is plotted as blue triangles, but also the nitrogen concentration estimated by SIMS is plotted as red circles, as shown in Figure 6(b). This nitrogen concentration was plot as a function of N/C gas ratio. The nearly identical values of [N] and [P1] indicate that most of the nitrogen is incorporated as N_s^0 which is substitutional nitrogen in the neutrally charged state. These data were aligned on a straight line (a straight line with a slope of 45 degrees on a log-log plot) over three orders of magnitude of nitrogen concentration. Finally, nitrogen concentration in diamond crystals was successfully controlled from 10 ppb to 10 ppm by changing the N/C gas ratio. A slop of this straight line corresponds to the incorporation efficiency, which is a ratio of [N_s^0] to N/C ratio in gas phase. The efficiency was estimated to be $(1.9\pm0.2)\times10^{-4}$. This value is two orders of magnitude lower than the incorporation efficiency using N_2O as a nitrogen source gas [41]. In this study, nitrogen doping was performed with molecular nitrogen under oxygen adding growth conditions. Constituent elements of the plasma in this study are hydrogen, carbon, oxygen, and nitrogen, which is the same as when N_2O is used as the nitrogen source gas. This fact suggests a difference of decomposition efficiency of nitrogen related gas in plasma affects the incorporation efficiency.

4. Formation of NV^- center in diamond

(a) Control of NV^- center concentration

The NV^- centers were formed using the following procedure. Electron beam irradiation is frequently used for creating vacancies in diamond [62, 63, 64], and heat treatment diffuses the vacancies [65, 66]. In this study, the grown HPHT and CVD diamonds were irradiated with a 2.0 MeV electron beam at about 300 K with a total fluence range from 1×10^{17} to 1×10^{18} electrons·cm^{-2}, with subsequent annealing at 1,000 °C for 2 h in vacuum [67]. Hereinafter, we designate this post process for NV^- center formation as “the e-beam/annealing process”. The [NV_T] examined for this study was 0.1–4 ppm. This value was controlled by the total fluence of an electron beam. [N_s^0] and [NV^-] before and after e-beam/annealing process were estimated by EPR measurements. For [NV^0] estimation, we first performed PL measurements to know the ratio [NV^0]/[NV^-]. Then by multiplying [NV^0]/[NV^-] in PL by [NV^-] in EPR, [NV^0] was obtained. Details on quantification can be found in the reference [68].

Figure 7 shows color change of diamond samples through the e-beam/annealing process. The color of as-grown HPHT diamond crystal was light yellowish, as shown in Fig. 7(a). The [N_s^0] of this HPHT synthetic diamond crystal was 6 ppm. When the crystals were treated by the e-beam/annealing process with a total fluence of 7×10^{17} electron·cm^{-2}, the color of the {111} growth sector near the crystal center turned purple, as shown in Fig. 7(b). The color of as-grown CVD diamond crystal was brownish, as shown in Fig. 7(c). The [N_s^0] of this CVD-grown diamond crystal was 11 ppm. After the e-beam/annealing process of the CVD diamond crystal with a total fluence of 3×10^{17} electron·cm^{-2}, the entire surface turned dark purple, as shown in Figure 7(d).

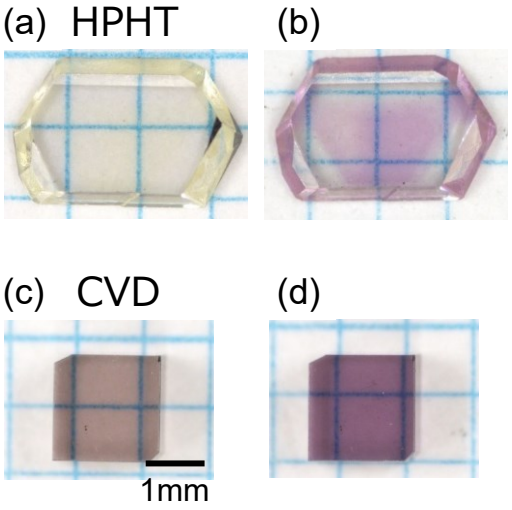

Figure 7. Color change of diamond samples through the e-beam/anneal process. HPHT samples (a) before and (b) after the process. CVD sample (c) before and (d) after the process.

As mentioned above, NV centers have different charge states, and negatively charged NV^- centers and neutral NV^0 centers are often observed simultaneously. The NV^0 centers increase significantly when the vacancy concentration in the diamond crystal becomes greater than the nitrogen concentration. This situation occurs when the diamond is overexposed to the electron beam [69, 70]. Therefore, it is necessary to determine the total fluence of electron beam so that the NV^- center becomes dominant. We clarified that the condition under which NV^- centers are predominantly formed is determined by the concentration ratio [NV_T]/[N_T] [68]. Here, [NV_T] = [NV^0] + [NV^-] and [N_T] is the initial [N_s^0] or [P1] before the formation of NV^- centers (*i.e.* before the e-beam/annealing process). We found that [NV^-] and the negative charge ratio of the NV centers [NV^-]/[NV_T] simultaneously become large values by setting [NV_T]/[N_T] to approximately 20% in our samples [68]. In the following experiments, the NV^- centers were formed such that the [NV_T]/[N_T] ratio was approximately 20%.

(b) Coherence time of NV^- centers

The spin-echo coherence time T_2 of the NV^- center was estimated using the Hahn echo pulse sequence [13, 71]. A home-built PL system with a pulsed microwave module was used for measurements [50, 72]. A 532-nm laser (gem 532; Laser Quantum Inc.) was used and the power density of the green laser at the specimen surface was set to 15 mW/μm^2. Figure 8(a) shows the T_2 of the NV^- centers as a function of concentration of nitrogen-related paramagnetic defects [N_{PM}]. Here, [N_{PM}] is the sum of [N_s^0] and [NV_T]. As described in the subsection 4 (a), [N_s^0], [NV^-] and [NV^0] were estimated by EPR and PL measurements [68]. Regarding concentration of NVH^- centers [NVH^-], EPR measurements have been performed. Here, ^{15}N enrichment of NVH^- centers are crucial for accurate concentration estimation of [NVH^-] [58, 72].

In Fig. 8, the measurement results for HPHT and CVD diamond crystals obtained in this study are plotted as red squares and red circles, respectively; the data for HPHT and CVD diamond crystals reported from Harvard University are plotted as open squares and open circles, respectively. A blue triangle shows the property for the HPHT diamond crystal with the highest AC magnetic sensitivity of 2.6 pT/√Hz reported from the University of Stuttgart [73]. Since the sensing time T_φ of 50 μs was described instead of T_2 in the reference [73], T_2 was inferred from an assumption that the magnetic-field sensitivity is maximum at $T_\varphi = T_2/2$. [N_{PM}] and [NV^-] of this sample in the reference [73] was 3 ppm and 0.9 ppm, respectively. The purple hexagon is a

measurement result of a commercially available diamond specimen from Element6 under the name DNV-B1. These data are distributed along a straight line, indicating a good inversely proportional relationship between T_2 and [N_{PM}]. Although there are multiple data for the same [N_{PM}] in the diamond crystal data grown at NIMS, it can be seen that they are distributed on an inversely proportional straight line with good reproducibility. This means that both the HPHT method and the CVD method can control [N_{PM}] by approximately two orders of magnitude.

There was no significant difference between the HPHT and CVD samples in this inversely proportional relationship. Compared to HPHT synthetic diamonds, CVD-grown diamonds generally contain hydrogen. In nitrogen-doped CVD diamond (001) single crystal, the hydrogen concentration is reportedly comparable to the nitrogen concentration in the crystal [58]. NVH^- centers are often formed in CVD diamond crystals by the incorporation of hydrogen, whose concentration is approximately 1/10 that of nitrogen [37, 49, 58]. Nevertheless, our results suggest that NVH^- centers do not affect T_2 of NV^- centers. Shinei *et al.* explain that the spin relaxation time of the NVH^- center is much shorter than that of the NV^- center and is therefore insufficient to disturb the spin coherence of the NV center$^-$ [72].

Figure 8(b) shows the T_2 of the ensemble NV^- centers as a function of concentration of NV^- centers. Similar to the [N_{PM}] dependence, T_2 was nearly inversely proportional to NV^- concentration [NV^-]. A similar tendency was observed because diamond crystals were irradiated with electron beams so that the conversion efficiency N_s^0 to NV^- was approximately 20%. Shot noise, which corresponds to the minimum detectable magnetic field, is inversely proportional to the square root of the product of the coherence time T_2 and concentration [NV^-]. The product of T_2 and [NV^-] of 66 and 75 μs ppm was obtained from two NIMS HPHT diamond. These values are close to the 90 μs ppm (blue triangle) reported by the University of Stuttgart, which represents the highest

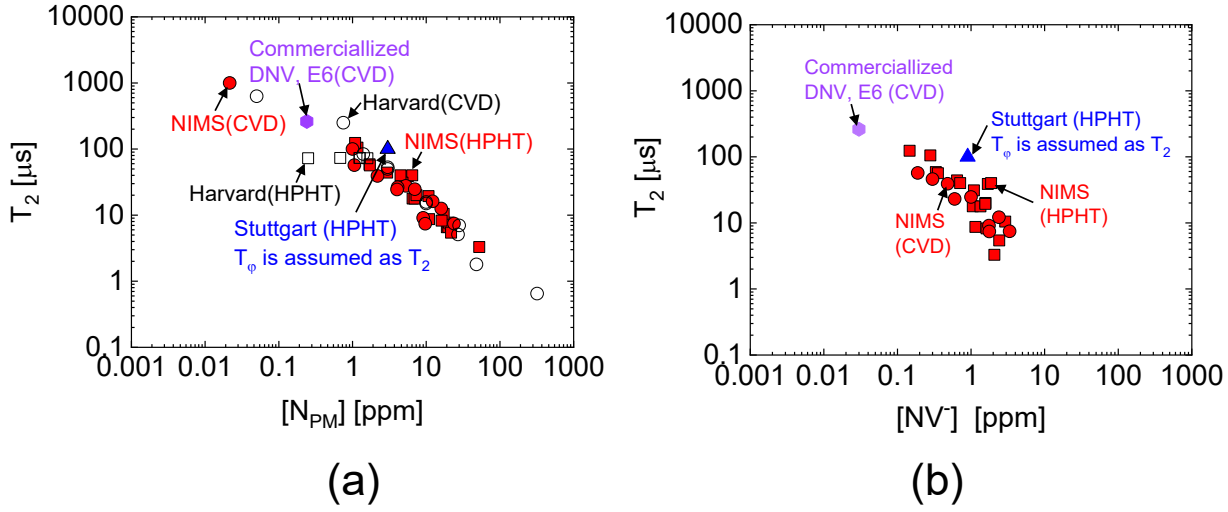

Figure 8. Coherence time of NV centers as a function of (a) nitrogen concentration [P1] and (b) negatively charged NV center concentration [NV^-]. As a references, data from Harvard university (open circles for CVD and open rectangles for HPHT diamond samples), data from university of Stuttgart (blue triangle for HPHT sample, sensing time T_φ of 50 μs was used for this plot assuming $T_2 = T_\varphi \times 2$.), sample commercialized from Element six (CVD sample named DNV-B1) were shown in the figures.

AC magnetic sensitivity to date [73]. This means that HPHT diamond crystals grown in NIMS are suitable for sensitive sensors, and we have techniques to prepare these diamond samples with higher reproducibility.

5. Summary

In this paper, we demonstrated high controllability of nitrogen concentration in diamond during crystal growth by HPHT and CVD methods. Chapter 2 described the principle of diamond crystal growth by HPHT and CVD methods, and the current status of nitrogen doping aimed at the preferential formation of NV^- centers. In Chapter 3, our research results in diamond crystal growth were described, focusing on the controllability of nitrogen doping concentration during diamond growth. We have succeeded in controlling the nitrogen concentration over two orders of magnitude. We showed that nitrogen concentration changed exponentially with the concentration of the nitrogen getter material in the HPHT method, and linearly with the nitrogen/carbon gas ratio in the CVD method. For HPHT crystals, a pair of {111} crystals were cut out from one grown crystal. In CVD diamond growth, it was demonstrated that isotope enrichment (^{12}C and ^{15}N) can be controlled in addition to nitrogen concentration control. As presented in Chapter 4, coherence time T_2 of NV^- centers of diamond prepared in this manner was inversely proportional to the concentration of nitrogen acting as a paramagnetic defect [N_{PM}] in the range of 1-50 ppm. A similar inverse relationship was found between T_2 and NV^- center concentration [NV^-]. The product of T_2 and [NV^-] is an indicator of magnetic field sensitivity, and this $T2 \cdot [NV^-]$ product obtained from our HPHT diamond crystals was comparable to that of the diamond crystal used for obtaining the highest AC magnetic sensitivities. The precise and reproducible nitrogen doping described in this paper is an important technique for designing highly sensitive magnetic sensor devices using NV^- centers.

Acknowledgments

Authors would like to thank Dr. H. Abe, Dr. S. Onoda, Dr. T. Ohshima of QST for supporting electron beam irradiation and Dr. H. Kanda for fruitful discussion. This work was partially supported by MEXT Q-LEAP (JPMXS0118068379 and JPMXS0118067395), JST CREST (JPMJCR1773), JST Moonshot R&D (JPMJMS2062), MIC R&D for construction of a global quantum cryptography network (JPMI00316), JSPS KAKENHI (No. 20H02187 and 20H05661).

References

1 Seskir, Z. C., Umbrello, S., Coenen, C. & Vermaas, P. E. 2023 Democratization of quantum technologies. Quantum Science and Technology 8. (DOI:10.1088/2058-9565/acb6ae).
2 Dowling, J. P. & Milburn, G. J. 2003 Quantum technology: the second quantum revolution. Philos Trans A Math Phys Eng Sci 361, 1655-1674. (DOI:10.1098/rsta.2003.1227).
3 Becher, C., Gao, W., Kar, S., Marciniak, C. D., Monz, T., Bartholomew, J. G., Goldner, P., Loh, H., Marcellina, E., Goh, K. E. J., et al. 2023 2023 roadmap for materials for quantum technologies. Materials for Quantum Technology 3. (DOI:10.1088/2633-4356/aca3f2).

4 Balasubramanian, G., Chan, I. Y., Kolesov, R., Al-Hmoud, M., Tisler, J., Shin, C., Kim, C., Wojcik, A., Hemmer, P. R., Krueger, A., et al. 2008 Nanoscale imaging magnetometry with diamond spins under ambient conditions. Nature 455, 648-651. (DOI:10.1038/nature07278).
5 Maze, J. R., Stanwix, P. L., Hodges, J. S., Hong, S., Taylor, J. M., Cappellaro, P., Jiang, L., Dutt, M. V., Togan, E., Zibrov, A. S., et al. 2008 Nanoscale magnetic sensing with an individual electronic spin in diamond. Nature 455, 644-647. (DOI:10.1038/nature07279).
6 Taylor, J. M., Cappellaro, P., Childress, L., Jiang, L., Budker, D., Hemmer, P. R., Yacoby, A., Walsworth, R. & Lukin, M. D. 2008 High-sensitivity diamond magnetometer with nanoscale resolution. Nat Phys 4, 810-816. (DOI:10.1038/nphys1075).
7 Aslam, N., Pfender, M., Neumann, P., Reuter, R., Zappe, A., Favaro de Oliveira, F., Denisenko, A., Sumiya, H., Onoda, S., Isoya, J., et al. 2017 Nanoscale nuclear magnetic resonance with chemical resolution. Science 357, 67-71. (DOI:10.1126/science.aam8697).
8 Hall, L. T., Simpson, D. A. & Hollenberg, L. C. L. 2013 Nanoscale sensing and imaging in biology using the nitrogen-vacancy center in diamond. Mrs Bull 38, 162-167. (DOI:10.1557/mrs.2013.24).
9 Hong, S., Grinolds, M. S., Pham, L. M., Le Sage, D., Luan, L., Walsworth, R. L. & Yacoby, A. 2013 Nanoscale magnetometry with NV centers in diamond. Mrs Bull 38, 155-161. (DOI:10.1557/mrs.2013.23).
10 Wrachtrup, J., Jelezko, F., Grotz, B. & McGuinness, L. 2013 Nitrogen-vacancy centers close to surfaces. Mrs Bull 38, 149-154. (DOI:10.1557/mrs.2013.22).
11 Gruber A, Drabenstedt A, Tietz C, Fleury L, Wrachtrup J, vonBorczyskowski C. 1997 Scanning confocal optical microscopy and magnetic resonance on single defect centers. *Science* 276, 2012-2014. (doi:10.1126/science.276.5321.2012).
12 Acosta, V. & Hemmer, P. 2013 Nitrogen-vacancy centers: Physics and applications. Mrs Bull 38, 127-133. (DOI:10.1557/mrs.2013.18).
13 Barry, J. F., Schloss, J. M., Bauch, E., Turner, M. J., Hart, C. A., Pham, L. M. & Walsworth, R. L. 2020 Sensitivity optimization for NV-diamond magnetometry. Rev Mod Phys 92. (DOI:ARTN 015004 10.1103/RevModPhys.92.015004).
14 Davies, R. C. B. a. G. J. 1992 Growth of synthetic diamond. In Properties of Natural and Synthetic Diamond (ed. J. E. Field), p. 395, Academic Press.
15 2018 The Global Diamond Industry 2018. (Antwerp World Diamond Centre and Bain & Company).
16 Kanda, H. 2000 Large Diamonds Grown at High Pressure Conditions. Braz J Phys 30, 482. (DOI: 10.1590/S0103-97332000000300003).
17 Burns, R. C. & Davies, G. J. 1992 Growth of synthetic diamond. In Properties of Natural and Synthetic Diamond (ed. J. E. Field), p. 395, Academic Press.
18 Setaka N. 1994 Development of Diamond Science and Technology in Japan. In *Synthetic Diamond Emerging CVD Science and Technology* (eds Spear K E, Dismukes J P) New York, US: John Wiley & Sons. ISBN 978-0471535898
19 Matsumoto S, Sato Y, Kamo M, Setaka N. 1982 Vapor-Deposition of Diamond Particles from Methane. *Japanese Journal of Applied Physics Part 2-Letters* 21, L183-L185. (doi:10.1143/Jjap.21.L183).
20 Kamo M, Sato Y, Matsumoto S, Setaka N. 1983 Diamond Synthesis from Gas-Phase in Microwave Plasma. *J Cryst Growth* 62, 642-644. (doi 10.1016/0022-0248(83)90411-6).
21 Sato, Y. & Kamo, M. 1992 Synthesis of diamond from the vapour phase. In Properties of Natural and Synthetic Diamond (ed. J. E. Field), p. 423, Academic Press.

22 Spear, K. E., Dismukes, John P. 1994 In Synthetic Diamond: Emerging CVD Science and Technology (John Wiley & Sons). ISBN 978-0081021835.
23 Teraji, T. 2008 Chemical Vapor Deposition of Homoepitaxial Diamond Films. In Physics and Applications of CVD Diamond (ed. C. N. Satoshi Koizumi, Milos Nesladek), pp. 29-75, Wiley-VCH Verlag GmbH & Co. KGaA.
24 Achard, J., Silva, F., Tallaire, A., Bonnin, X., Lombardi, G., Hassouni, K. & Gicquel, A. 2007 High quality MPACVD diamond single crystal growth: high microwave power density regime. J Phys D Appl Phys 40, 6175-6188. (DOI:10.1088/0022-3727/40/20/S04).
25 Achard, J., Arnault, J.-C., Chayahara, A., Hatano, M., Iwasaki, T., Mokuno, Y., Schreck, M., Tallaire, A., Teraji, T., Tokuda, N., et al. 2018 Diamond wafer technologies for semiconductor device applications. In Woodh Pub Ser Elect (eds. S. Koizumi, H. Umezawa, J. Pernot & M. Suzuki), pp. 1-97, Woodhead Publishing.
26 Goss, J. P., Eyre, R. J. & Briddon, P. R. 2008 Theoretical Models for Doping Diamond for Semiconductor Applications. In Physics and Applications of CVD Diamond (pp. 199-236.
27 Achard, J., Issaoui, R., Tallaire, A., Silva, F., Barjon, J., Jomard, F. & Gicquel, A. 2012 Freestanding CVD boron doped diamond single crystals: A substrate for vertical power electronic devices? physica status solidi (a) 209, 1651-1658. (DOI:10.1002/pssa.201200045).
28 Burns, R. C., Hansen, J. O., Spits, R. A., Sibanda, M., Welbourn, C. M. & Welch, D. L. 1999 Growth of high purity large synthetic diamond crystals. Diam Relat Mater 8, 1433-1437. (DOI:10.1016/s0925-9635(99)00042-4).
29 Miyakawa M, Shinei C, Taniguchi T. 2022 Nitrogen concentration control in diamonds grown in Co-(Fe)-Ti/Al solvents under high-pressure and high-temperature. *Japanese Journal of Applied Physics* 61. 045507 1-4 (doi:10.35848/1347-4065/ac5d7f).
30 Sumiya H, Tamasaku K 2012 Large Defect-Free Synthetic Type IIa Diamond Crystals Synthesized via High Pressure and High Temperature. *Japanese Journal of Applied Physics* 51, 045507 1-4 (doi:10.1143/Jjap.51.090102).
31 Sumiya H, Toda N, Nishibayashi Y, Satoh S. 1997 Crystalline perfection of high purity synthetic diamond crystal. J Cryst Growth 178, 485-494. (doi:10.1016/s0022-0248(96)00797-x).
32 Liang, Z. Z., Jia, X., Ma, H. A., Zang, C. Y., Zhu, P. W., Guan, Q. F. & Kanda, H. 2005 Synthesis of HPHT diamond containing high concentrations of nitrogen impurities using NaN3 as dopant in metal-carbon system. Diam Relat Mater 14, 1932-1935. (DOI:10.1016/j.diamond.2005.06.041).
33 Clark C D, Collins A T, Woods G S. 1992 Absorption and luminescence spectroscopy. In *Properties of Natural and Synthetic Diamond* (eds Field J E) London, UK: Academic Press. ISBN 978-0122553523.
34 Zaitsev, A. M. 2001 Optical Properties of Diamond: A Data Handbook, Springer.
35 Teraji T, Taniguchi T, Koizumi S, Koide Y, Isoya J. 2013 Effective Use of Source Gas for Diamond Growth with Isotopic Enrichment. *Appl Phys Express* 6. (doi:10.7567/Apex.6.055601).
36 Chayahara, A., Mokuno, Y., Horino, Y., Takasu, Y., Kato, H., Yoshikawa, H. & Fujimori, N. 2004 The effect of nitrogen addition during high-rate homoepitaxial growth of diamond by microwave plasma CVD. Diam Relat Mater 13, 1954-1958. (DOI:10.1016/j.diamond.2004.07.007).
37 Tallaire, A., Collins, A. T., Charles, D., Achard, J., Sussmann, R., Gicquel, A., Newton, M. E., Edmonds, A. M. & Cruddace, R. J. 2006 Characterisation of high-quality thick single-crystal diamond grown by CVD with a low nitrogen addition. Diam Relat Mater 15, 1700-1707. (DOI:10.1016/j.diamond.2006.02.005).
38 Watanabe H, Kitamura T, Nakashima S, Shikata S 2009 Cathodoluminescence characterization of a nitrogen-doped homoepitaxial diamond thin film. *J Appl Phys* 105. (doi:10.1063/1.3117214).
39 Yan, C. S., Vohra, Y. K., Mao, H. K. & Hemley, R. J. 2002 Very high growth rate chemical vapor deposition of single-crystal diamond. Proc Natl Acad Sci U S A 99, 12523-12525. (DOI:10.1073/pnas.152464799).

40 Tallaire, A., Brinza, O., Huillery, P., Delord, T., Pellet-Mary, C., Staacke, R., Abel, B., Pezzagna, S., Meijer, J., Touati, N., et al. 2020 High NV density in a pink CVD diamond grown with N2O addition. Carbon 170, 421-429. (DOI:10.1016/j.carbon.2020.08.048).
41 Tallaire, A., Mayer, L., Brinza, O., Pinault-Thaury, M. A., Debuisschert, T. & Achard, J. 2017 Highly photostable NV centre ensembles in CVD diamond produced by using N2O as the doping gas. Applied Physics Letters 111. (DOI:10.1063/1.5004106).
42 Tsuji, T., Ishiwata, H., Sekiguchi, T., Iwasaki, T. & Hatano, M. 2022 High growth rate synthesis of diamond film containing perfectly aligned nitrogen-vacancy centers by high-power density plasma CVD. Diam Relat Mater 123. (DOI:10.1016/j.diamond.2022.108840).
43 de Theije, F. K., Schermer, J. J. & van Enckevort, W. J. P. 2000 Effects of nitrogen impurities on the CVD growth of diamond: step bunching in theory and experiment. Diam Relat Mater 9, 1439-1449. (DOI:10.1016/s0925-9635(00)00261-2).
44 Tallaire, A., Achard, J., Silva, F., Sussmann, R. S. & Gicquel, A. 2005 Homoepitaxial deposition of high-quality thick diamond films: effect of growth parameters. Diam Relat Mater 14, 249-254. (DOI:10.1016/j.diamond.2004.10.037).
45 Ashfold M N R, Goss J P, Green B L, May P W, Newton M E, and Peaker C V. 2020 Nitrogen in Diamond *Chemical Reviews* 120, 5745-5794. (10.1021/acs.chemrev.9b00518).
46 Chayahara, A., Mokuno, Y., Horino, Y., Takasu, Y., Kato, H., Yoshikawa, H. & Fujimori, N. 2004 The effect of nitrogen addition during high-rate homoepitaxial growth of diamond by microwave plasma CVD. Diam Relat Mater 13, 1954-1958. (DOI:10.1016/j.diamond.2004.07.007).
47 Meng, Y. F., Yan, C. S., Lai, J., Krasnicki, S., Shu, H., Yu, T., Liang, Q., Mao, H. K. & Hemley, R. J. 2008 Enhanced optical properties of chemical vapor deposited single crystal diamond by low-pressure/high-temperature annealing. Proc Natl Acad Sci U S A 105, 17620-17625. (DOI:10.1073/pnas.0808230105).
48 Zaitsev, A. M., Kazuchits, N. M., Moe, K. S., Butler, J. E., Korolik, O. V., Rusetsky, M. S. & Kazuchits, V. N. 2021 Luminescence of brown CVD diamond: 468 nm luminescence center. Diam Relat Mater 113. (DOI:ARTN 108255
10.1016/j.diamond.2021.108255).
49 Edmonds, A. M., D'Haenens-Johansson, U. F. S., Cruddace, R. J., Newton, M. E., Fu, K. M. C., Santori, C., Beausoleil, R. G., Twitchen, D. J. & Markham, M. L. 2012 Production of oriented nitrogen-vacancy color centers in synthetic diamond. Physical Review B 86. (DOI:ARTN 035201
10.1103/PhysRevB.86.035201).
50 Masuyama Y, Shinei C, Ishii S, Abe H, Taniguchi T, Teraji T, Ohshima T, 2023, *arXiv*:2301.12441.
51 Hatano, M. 2022 Potential of diamond solid-state quantum sensors. In 2022 International Electron Devices Meeting (IEDM) (pp. 14.15.11-14.15.14.
52 Stoneham A M. 1992 Diamond: Recent Advances in Theory. In *Properties of Natural and Synthetic Diamond* (eds Field J E) London, UK: Academic Press. ISBN 978-0122553523.
53 Zaitsev A M. 2001 *Optical Properties of Diamond: A Data Handbook*. Berlin, Germany: Springer. ISBN 978-3540665823
54 Mizuochi N, Neumann P, Rempp F, Beck J, Jacques V, Siyushev P, Nakamura K, Twitchen D J, Watanabe H, Yamasaki S, Jelezko F, Wrachtrup J. 2009 Coherence of single spins coupled to a nuclear spin bath of varying density. *Physical Review B* 80. (doi:10.1103/PhysRevB.80.041201).

55 Jahnke K D, Naydenov B, Teraji T, Koizumi S, Umeda T, Isoya J, Jelezko F. 2012 Long coherence time of spin qubits in C-12 enriched polycrystalline chemical vapor deposition diamond. *Applied Physics Letters* 101. (doi:10.1063/1.4731778).
56 Sumiya H, Satoh S 1996 High-pressure synthesis of high-purity diamond crystal. *Diam Relat Mater* 5, 1359-1365. (doi:10.1016/0925-9635(96)00559-6).
57 Yamaoka S, Akaishi M, Kanda H, Osawa T 1992 Crystal growth of diamond in the system of carbon and water under very high pressure and temperature. *J Cryst Growth* 125, 375-377. (doi:10.1016/0022-0248(92)90351-i).
58 Teraji, T. & Shinei, C. 2023 Nitrogen-related point defects in homoepitaxial diamond (001) freestanding single crystals. J Appl Phys 133. (DOI:10.1063/5.0143652).
59 Teraji T, Yamamoto T, Watanabe K, Koide Y, Isoya J, Onoda S, Ohshima T, Rogers L J, Jelezko F, Neumann P, Wrachtrup J, Koizumi S. 2015 Homoepitaxial diamond film growth: High purity, high crystalline quality, isotopic enrichment, and single color center formation. *Phys Status Solidi A* 212, 2365-2384. (doi:10.1002/pssa.201532449).
60 Teraji T, Isoya J, Watanabe K, Koizumi S, Koide Y, 2017 Homoepitaxial diamond chemical vapor deposition for ultra-light doping, *Materials Science in Semiconductor Processing* 70, 197-202. (doi: 10.1016/j.mssp.2016.11.012).
61 Burns R C, Cvetkovic V, Dodge C N, Evans D J F, Rooney M-L T, Spear P M, Welbourn C M. 1990 Growth-sector dependence of optical features in large synthetic diamonds *J. Cryst. Growth* 104, 257-279 (doi: 10.1016/0022-0248(90)90126-6).
62 Campbell, B. & Mainwood, A. 2000 Radiation Damage of Diamond by Electron and Gamma Irradiation. physica status solidi (a) 181, 99-107. (DOI:10.1002/1521-396x(200009)181:1<99::Aid-pssa99>3.0.Co;2-5).
63 Twitchen, D. J., Newton, M. E., Baker, J. M., Anthony, T. R. & Banholzer, W. F. 1999 Electron-paramagnetic-resonance measurements on the divacancy defect center R4/W6 in diamond. Physical Review B 59, 12900-12910. (DOI:DOI 10.1103/PhysRevB.59.12900).
64 Acosta, V. M., Bauch, E., Ledbetter, M. P., Santori, C., Fu, K. M. C., Barclay, P. E., Beausoleil, R. G., Linget, H., Roch, J. F., Treussart, F., et al. 2009 Diamonds with a high density of nitrogen-vacancy centers for magnetometry applications. Physical Review B 80. (DOI:ARTN 115202 10.1103/PhysRevB.80.115202).
65 Breuer, S. J. & Briddon, P. R. 1995 Ab initio investigation of the native defects in diamond and self-diffusion. Physical review. B, Condensed matter 51, 6984-6994. (DOI:10.1103/physrevb.51.6984).
66 Davies, G., Lawson, S. C., Collins, A. T., Mainwood, A. & Sharp, S. J. 1992 Vacancy-related centers in diamond. Physical review. B, Condensed matter 46, 13157-13170. (DOI:10.1103/physrevb.46.13157).
67 Ishii, S., Saiki, S., Onoda, S., Masuyama, Y., Abe, H. & Ohshima, T. 2021 Ensemble Negatively-Charged Nitrogen-Vacancy Centers in Type-Ib Diamond Created by High Fluence Electron Beam Irradiation. Quantum Beam Science 6. (DOI:10.3390/qubs6010002).
68 Shinei C, Miyakawa M, Ishii S, Saiki S, Onoda S, Taniguchi T, Ohshima T, Teraji T. 2021 Equilibrium charge state of NV centers in diamond. *Applied Physics Letters* 119, 254001. (doi:10.1063/5.0079687).
69 Waldermann F C, Olivero P, Nunn J, Surmacz K, Wang Z Y, Jaksch D, Taylor R A, Walmsley I A, Draganski M, Reichart P, Greentree A D, Jamieson D N and Prawer S. 2007 Creating diamond color centers for quantum optical applications. *Diam Relat Mater* 16, 1887-1895. (doi:10.1016/j.diamond.2007.09.009).
70 Luo, T., Lindner, L., Langer, J., Cimalla, V., Vidal, X., Hahl, F., Schreyvogel, C., Onoda, S., Ishii, S., Ohshima, T., et al. 2022 Creation of nitrogen-vacancy centers in chemical vapor deposition diamond for sensing applications. New J Phys 24. (DOI:10.1088/1367-2630/ac58b6).
71 Hahn, E. L. 1950 Spin Echoes. Physical Review 80, 580-594. (DOI:10.1103/PhysRev.80.580).

72 Shinei, C., Masuyama, Y., Miyakawa, M., Abe, H., Ishii, S., Saiki, S., Onoda, S., Taniguchi, T., Ohshima, T. & Teraji, T. 2022 Nitrogen related paramagnetic defects: Decoherence source of ensemble of NV- center. *J Appl Phys* 132, 214402 1-11 (doi:10.1063/5.0103332).
73 Wolf, T., Neumann, P., Nakamura, K., Sumiya, H., Ohshima, T., Isoya, J. & Wrachtrup, J. 2015 Subpicotesla Diamond Magnetometry. Phys Rev X 5. (DOI:ARTN 041001 10.1103/PhysRevX.5.041001).